Food and Chemical Toxicology 124 (2019) 336–348

Contents lists available at ScienceDirect

Food and Chemical Toxicology

journal homepage: www.elsevier.com/locate/foodchemtox

Corynoxine B ameliorates HMGB1-dependent autophagy dysfunction during manganese exposure in SH-SY5Y human neuroblastoma cells

Dongying Yan, Zhuo Ma, Chang Liu, Can Wang, Yu Deng, Wei Liu, Bin Xu*

Department of Environmental Health, School of Public Health, China Medical University, No.77 Puhe Road, Shenyang North New Area, Shenyang, Liaoning Province, 110122, PR China

ARTICLE INFO

Keywords:
Manganese
Alpha-synuclein
Autophagy
Neurotoxicity
HMGB1
Corynoxine B

ABSTRACT

Manganese (Mn) has recently come into the limelight as an important environmental risk factor for neurodegenerative disorders. Although multiple neurotoxicity of Mn have been extensively studied, the exact mechanism of Mn-induced autophagic dysregulation is still poorly understood. The main aim of this study was to explore the role of cytosolic high-mobility group box 1 (HMGB1)-dependent autophagy in Mn-induced autophagic dysregulation and neurotoxicity. SH-SY5Y cells were treated with culture solution (control) and three different concentrations of Mn (50, 100, and 200 μM) for 24 h to detect the effect of Mn on HMGB1-dependent autophagy. We found Mn could increase the HMGB1 mRNA level and its cytosolic translocation and dysregulate autophagy, and Mn-induced alpha-synuclein overexpression interfered with the interaction of HMGB1 and Beclin1, to subsequently promote Beclin1 binding to Bcl2. Another important finding was the neuroprotective role of corynoxine B (Cory B) in Mn-induced autophagic dysregulation and neurotoxicity. We set up six experimental groups: control (culture solution); 200 μM Mn treatment; 100 μM Cory B-alone treatment; and three different pretreated concentrations of Cory B (25, 50, and 100 μM). Our results showed that Cory B ameliorated Mn-induced autophagic dysregulation and neurotoxicity partly by dissociating HMGB1 from alpha-synuclein and inhibiting mTOR signaling.

1. Introduction

Manganese (Mn)—an essential trace element in humans—is ubiquitous in the earth's crust and plays an important role in brain physiology and homeostasis (Chen et al., 2015; O'Neal and Zheng, 2015). However, chronic overexposure to Mn can cause neurotoxicity resulting in neurodegenerative disease, referred to as manganism, which features symptomatology similar to Parkinson's disease (PD) (Chen et al., 2015). Excess Mn exposure is a common occupational hazard in Mn mining and smelting, steel production, and battery manufacturing (O'Neal and Zheng, 2015). Epidemiological studies have revealed that a high environmental level of Mn is closely associated with increased risk for Parkinsonian-like symptoms (O'Neal and Zheng, 2015). Therefore, Mn is an environmental pathogenic factor for neurodegenerative diseases.

Autophagy (hereby referred as to macroautophagy) is a highly conservative biological degradation and recycling pathway for maintaining cellular homeostasis (Murrow and Debnath, 2013; Zhang et al., 2016). Autophagy that occurs at low basal levels under the physiological state can be activated in response to pathological stimuli by H_2O_2, rapamycin, endoplasmic reticulum (ER) stress, and hypoxia (Murrow and Debnath, 2013). Emerging evidence indicates that autophagy is essential for neural function and plays a neuroprotective role. In addition, current literature provides evidence that dysfunction of autophagy (suppression or excessive activation) is closely associated with development of neurodegenerative diseases (Lynch-Day et al., 2012; Zhang et al., 2016). Recently, increasing evidence suggests that Mn exposure causes dysfunction of autophagy (Yuan et al., 2016; Zhang et al., 2013). Yet, the exact mechanism of Mn affecting autophagy remains poorly understood.

Induction of autophagy can be regulated by multiple signaling pathways such as mTOR-ULK and Beclin1-PIK3C3 (Jin and Klionsky, 2014; Ravanan et al., 2017). Beclin1 (Atg6), as an important autophagy protein, is indispensable for autophagy induction. Originally, Beclin1 was identified as an interaction partner for Bcl-2—an anti-apoptotic protein. Some studies report that Beclin1 plays a critical role in the regulation of autophagy by interacting with various cofactors such as Atg14L, UVRAG, Bif-1, Vsp34, and HMGB1 (Kang et al., 2011; Wirawan et al., 2012). High-mobility group box 1 (HMGB1), as a highly conserved nuclear protein and damage-associated molecular pattern (DAMP) molecule, is a 215-aa protein of ~30 kDa and stored in the

* Corresponding author.
E-mail address: bxu10@cmu.edu.cn (B. Xu).

https://doi.org/10.1016/j.fct.2018.12.027
Received 12 October 2018; Received in revised form 27 November 2018; Accepted 18 December 2018
Available online 19 December 2018
0278-6915/

nucleus under physiological conditions. Structurally, HMGB1 is composed of three domains: two positively charged domains (A box and B box) and a negatively charged carboxyl terminus (the acidic tail) (Yu et al., 2015). Recent studies have shown that HMGB1 exerts multiple biological functions both intracellularly and extracellularly (Tang et al., 2011); in the latter, HMGB1 functions as an extracellular signaling molecule accompanied by its nuclear-to-cytosolic translocation during inflammation, trauma, necrosis, and oxidative and metabolic stress (Tang et al., 2011). It has been reported that endogenous HMGB1 acts as a novel Beclin1-binding protein, being involved in the regulation of autophagy (Kang et al., 2010). Moreover, the involvement of HMGB1 has been recently indicated in the process of autophagic impairment by overexpression of alpha-synuclein (α-SYN) (Wang et al., 2016). Our team has confirmed that α-SYN overexpression or oligomerization is a pathogenic feature and also a causative factor upon Mn-induced neurotoxicity via multiple pathogenic mechanisms such as endoplasmic reticulum (ER) stress, autophagic dysfunction, etc. (Xu et al., 2013, 2014a, 2014b, 2015). Based on these findings, we hypothesized that there is a potential molecular mechanism for Mn-induced α-SYN overexpression that disturbs HMGB1-dependent autophagy.

Originally, patients of manganism were treated with levodopa, however, they were unresponsive to the treatment. Hopefully, Corynoxine B (Cory B) from *Uncaria rhynchophylla* (Miq.) Jacks (Gouteng in Chinese)—a Beclin1-dependent autophagy inducer—plays an important neuroprotective role in a wide range of neuronal cells (Chen et al., 2014). Classical autophagy inducers such as starvation, rapamycin, and everolimus always affect some signaling pathways including Akt, JNK, and PERK in the activation of autophagy. In contrast, Cory B has no effects on the above-mentioned pathways (Chen et al., 2014). Hence, Cory B may be a potent means to regulate autophagy by exerting preventive and therapeutic role against neurodegenerative diseases such as manganism.

In this study, we provided evidence for the pivotal role of HMGB1 in Mn-induced autophagic dysregulation. Additionally, we demonstrated the neuroprotective role of Cory B in ameliorating Mn-induced autophagic inhibition and neurotoxicity in SH-SY5Y cells, which was partly attributed to dissociation of HMGB1 from alpha-synuclein and mTOR signaling inhibition.

2. Materials and methods

2.1. Chemicals

SH-SY5Y cells were obtained from American Type Culture Collection (ATCC, CRL-2266). Cory B was purchased from MedChem Express (# HY-17391, NJ, USA). Manganese (II) chloride tetrahydrate was obtained from Sigma Chemical Co. (St. Louis, MO, USA). Annexin V-FITC/PI reagent kit was purchased from Nanjing KeyGen Biotech. Co. Ltd. (# KGA 106, China). *PrimeScript*® RT Enzyme Mix I and SYBR® Premix Ex *Taq*™ II kits were purchased from TaKaRa Biotech. Co. Ltd. Ad-mCherry-GFP-LC3B was purchased from Beyotime Biotechnology (#C3011, Shanghai, China). BeaverBeads™Magrose Strep-Tactin was supplied by BEAVER (# 70808-5, Suzhou, China). Rabbit dylight 488 conjugated HMGB1 and mouse α-SYN primary antibodies were purchased from Thermo Fisher Scientific. Rabbit mTOR, rabbit p-mTOR, and rabbit LMNB1 primary antibodies were purchased from Cell Signaling Technology (Danvers, MA, USA). Rabbit LC3B, p62, 4EBP1, p-4EBP1, p-S6K1, S6K1, α-SYN, HMGB1, and β-actin primary antibodies were purchased from Abclonal Biotechnology Co. Ltd. Rabbit Beclin1, mouse Bcl2, and mouse HMGB1 primary antibodies were purchased from Abcam Ltd. (Hong Kong). Horseradish peroxidase (HRP)-conjugated anti-rabbit secondary antibody and HRP-conjugated anti-mouse secondary antibody were purchased from Abcam. Cy3-conjugated goat anti-mouse IgG (# GB21301) and FITC-conjugated goat anti-rabbit IgG (# GB22303) were purchased from Servicebio. (Wuhan, China). Other chemicals of analytical grade used in our study were supplied by local chemical suppliers.

2.2. Cells culture and treatments

SH-SY5Y cells were cultured in a 1:1 mixture of Ham's F12 medium and Dulbecco's Modified Eagle's Medium (DMEM) supplemented with 10% FBS (Cergy-Pontoise, France) and 100 U/ml penicillin/streptomycin (Cergy-Pontoise, France) and seeded in cell culture flasks at an initial density of 1×10^5 cells/ml. Cells were incubated at 37 °C in a humidified atmosphere of 5% CO_2 for 3 days until they reached 80% confluence, and then treated with test chemicals. SH-SY5Y cells were individually treated with 50, 100, and 200 μM $MnCl_2$ or culture solution (control) for 24 h and were subsequently used for detection as relative indicators. In addition, we used Cory B autophagy inducer to explore the molecular mechanism in Mn-induced neurotoxicity. In detail, SH-SH5Y cell cultures were divided into the following six experimental groups: culture solution (control); 200 μM Mn treatment; 100 μM Cory B-alone treatment; and three different concentrations of Cory B (25, 50, and 100 μM) pretreatments, incubated for 2 h before 200 μM Mn treatment. After incubation for 24 h at 37 °C in 5% (v/v) CO_2, cells were collected to detect relative indication.

2.3. Cell viability and LDH assay

Cell viability was detected using the Cell Counting Kit (CCK)-8 assay according to the manufacturer's instruction (Beyotime Biotechnology). Briefly, SH-SY5Y cells were seeded in 96-well plates at 5×10^4 cells/well and incubated for 24–48 h before chemical treatments. After above-described treatments, the absorbance value of each well was measured at 450 nm with a microplate reader.

Levels of lactate dehydrogenase (LDH) release in the cell culture medium are commonly used to assess cytotoxicity. The release level of LDH was measured using an LDH Kit (Beyotime Biotechnology) according to the manufacturer's protocol.

2.4. Western blotting assay

To assess HMGB1 expression, we extracted nuclear and cytoplasmic proteins by using a Nuclear and Cytoplasmic Extraction Reagents Kit (Beyotime Biotechnology) according to the product's manual. Expression in whole-cell lysates was evaluated for autophagic related proteins, mTOR downstream proteins, α-SYN, and Bcl2. After concentration normalization to 2 μg/μl using bicinchoninic acid (BCA) reagent (#23227, Thermo Fisher, IL, USA), approximately 20 μg proteins were loaded onto 12% or 6% SDS-polyacrylamide gels, then electrotransferred onto PVDF membranes. After blockage with 5% albumin from bovine serum (BSA) solution, the membranes were incubated overnight at 4 °C with the following primary antibodies: Beclin1, LC3B, p62, α-SYN, Bcl2, mTOR, p-mTOR, 4EBP1, p-4EBP1, S6K1, p-S6K1, HMGB1, LMNB1, and β-actin antibody. Afterwards, the membranes were incubated with HRP-conjugated anti-rabbit or anti-mouse secondary antibodies. An ECL chemiluminescent system (C300, Azure, USA) was used to detect the protein bands. Relative gray intensities were quantified using Image J software (Image J, NIH, Bethesda, MA, USA).

2.5. Apoptosis assays

After the indicated treatments, the harvested cells were stained with Annexin V-FITC and propidium iodide (PI) according to the manufacturer's instructions (Nanjing KeyGen Biotech. Co. Ltd.). The resulting fluorescence was detected by using a flow cytometer (BD FACSCantoCantoII, USA), and single-positive cells (Annexin V^+/PI^-, Q4) were considered as indicators of early apoptosis.

2.6. Detection of autophagic vacuoles by MDC staining and flow cytometry

After culture in 48-well plates for 24 h, cells were treated as previously indicated. Then, the cells were stained with 50 mM monodansylcadaverine (MDC) (# 10121, SIGMA) in medium containing 10% FBS at 37 °C for 45 min in dark and washed twice with warm PBS. Images were captured under inverted fluorescence microscope. To quantify the MDC-labeled positive autophagic vacuoles, cells were harvested after indicated treatments, and the fluorescent signals were detected by flow cytometry (BD FACSCantoCantoII, USA). Mean fluorescence intensity reflected the level of autophagy occurrence.

2.7. Immunofluorescent staining and confocal microscopic analysis

After indicated treatments, SH-SY5Y cells were seeded on 35-mm culture plates and fixed with 4% paraformaldehyde for 15 min, penetrated with 0.2% TritonX-100 for 20 min, and blocked with 5% goat serum albumin for 30 min at room temperature. Afterwards, cells were single stained with dylight 488 conjugated HMGB1 (rabbit, 1:100, Thermo Fisher Scientific), double stained with anti-HMGB1 (rabbit, 1:100, Abclonal Biotechnology) and α-SYN (mouse, 1:100, Thermo Fisher Scientific), double stained with anti-HMGB1 (mouse, 1:100, Abcam Ltd.) and Beclin1 (rabbit, 1:100, Abcam Ltd.), and double stained with anti-Beclin1 (rabbit, 1:100, Abcam Ltd.) and Bcl2 (mouse, 1:100, Abcam Ltd.) antibodies overnight at 4 °C, followed by Cy3-conjugated goat anti-mouse IgG and FITC-conjugated goat anti-rabbit IgG secondary antibodies (1:500). After three washes, cells were incubated with DAPI for 5 min in the dark and viewed under an Olympus laser confocal microscope (×40, FV 1000S-IX81, Olympus, Japan). The results were analyzed via calculating the Pearson's correlation coefficient or yellow dots by Image J to quantify HMGB1 cytosolic translocation, the colocalization of HMGB1 and α-SYN, HMGB1 and Beclin1, and Beclin1 and Bcl2 (Zinchuk et al., 2007). In majority of cases, Pearson's correlation coefficient could describe the correlation of the intensity distribution between channels. The following was used to calculate Pearson's correlation coefficient by Image J software: 1) Images saved in TIFF format should be transform into 8-bit images (Image-Type-8-bit); 2) Single channel of image (green channel or red channel) were splited (edit, copy-dile, new, internal clipboard, internal clipboard-1); 3) Pearson's correlation coefficient and scatter gram were measured (Plugin-colocalization finder).

2.8. Co-immunoprecipitation assay (Co-IP)

After the indicated treatments, cytoplasmic proteins were extracted from SH-SY5Y cells by using a cytoplasmic extraction reagents kit (Beyotime Biotechnology). After cytoplasmic protein concentration was normalized to 2 μg/μl, we used Beclin1 (rabbit, 1:40, Abcam Ltd.) or HMGB1 (α-SYN) primary antibody to selectively precipitate the antigen complex at 4 °C overnight. Then, the antigen-antibody complex was incubated with 25 μl of immunomagnetic beads for 2 h. Next, the beads-antigen-antibody complex was used for western blotting, as described above. The membrane blots were blotted with the appropriate primary antibodies followed by secondary antibodies; the blots were then visualized by chemiluminescent detection reagents (Pierce).

2.9. Quantitative real-time PCR analysis

mRNA samples from SH-SY5Y cells were obtained using Trizol reagent (TaKaRa Biotech. Co. Ltd., China), and reverse transcription was performed with PrimeScript® RT Enzyme Mix I (TaKaRa Biotech. Co. Ltd., China) and oligo (dT) primers according to the manufacturer's protocol. Real-time quantitative PCR was performed with SYBR® Premix Ex TaqTM II kit (TaKaRa Biotech. Co. Ltd., China) using an ABI 7500 Real-Time PCR System (Applied Biosystems, USA). The final volume of the reaction mixture was 20 μl, and the real-time PCR assay was performed at 95 °C for 5 s, 60 °C for 34 s, and 72 °C for 20 s for the PCR reaction, with 40-cycles. The following PCR primers were used: HMGB1, 5′-GGAGATCCTAAGAAGCCGAGA (forward) and 5′-CATGGT CTTCCACCTCTCTGA (reverse); and β-actin, 5′-CCAACCGCGAGAAGA TGA (forward) and 5′-CCAGAGGCGTACAGGGATAG (reverse). The mRNA level was normalized to endogenous control β-actin, with the $2^{-\Delta\Delta Ct}$ method.

2.10. Ad-mCherry-CFP-LC3B transfection

SH-SY5Y cells were seeded in 6-well plates at 5×10^5 cells/well for 24 h and reached 20%–30% confluence at the time of transfection. Cells were transfected with Ad-mCherry-GFP-LC3B adenovirus at a multiplicity of infection (MOI) of 80 in 800 μl in medium containing 10% FBS at 37 °C for 24 h. After the indicated treatments, a laser scanning confocal microscope (×60, FV 1000S-IX81, Olympus, Japan) was used to observe the changes of autophagy flux. The number of red and yellow LC3 dots per cell were counted under confocal microscope (> 10 cells/group).

2.11. Statistical analysis

Statistical analysis was performed by one-way ANOVA followed by the Student-Newman-Keuls test (*q*-test). All data are presented as means ± standard deviation. Pearson's correlation coefficient was calculated by Image J. A p-value < 0.05 was set as statistically significant.

3. Results

3.1. Mn exposure induced cytosolic translocation of HMGB1 and activated autophagy via HMGB1-Beclin1 binding

In terms of the cytosolic role, HMGB1 can translocate from the nucleus into cytosol during pathological stress and subsequently become involved in the regulation of autophagy (Sun and Tang, 2014). Accordingly, laser confocal microscopy showed that HMGB1 was mainly present in the nucleus in control SH-SY5Y cells and its cytosolic translocation was generally enhanced in 100 and 200 μM Mn-treated SH-SY5Y cells evidenced by a decrease in Pearson's correlation coefficient (merged by HMGB1-dylight 488 and nuclei-DAPI) (Fig. 1a). Similarly, the expression of HMGB1 was significantly increased in the cytosolic fraction of 100 and 200 μM Mn-treated SH-SY5Y cells compared to the control, while there was no obvious change in the nuclear fraction (Fig. 1b). Besides, we also found that Mn (100, 200 μM) treatment significantly increased the HMGB1 mRNA level ($p < 0.05$; Fig. 1c). By immunofluorescence and Co-IP experiments, we demonstrated that Mn obviously enhanced the colocalization (yellow dots merged by HMGB1-Cy3 and Beclin1-FITC) and interaction of HMGB1 and Beclin1 accompanied by the increase of cytosolic translocation of HMGB1 compared to the control (Fig. 1d and e). However, in 100 μM Mn-treated SH-SY5Y cells, this binding greatly increased to more than that in the 200 μM Mn-treated cells (Fig. 1e), suggesting that Mn overexposure could weaken the HMGB1-Beclin1 interaction.

To further confirm the effect of Mn on autophagy, inverted fluorescence microscopy and flow cytometry were used to observe and quantify MDC-labeled positive autophagic vacuoles in SH-SY5Y cells. The positive dots and mean fluorescence intensity were enhanced after Mn treatment (50–200 μM) (Fig. 2a and b). Notably, the enhanced effect appeared more conspicuously in 100 μM Mn treatment than that in 200 μM Mn treatment. Next, we transiently transfected SH-SY5Y cells with Ad-mCherry-GFP-LC3B adenovirus to evaluate the state of autophagy flux. In general, green fluorescence, an acid-sensitive protein, was quenched when autophagosomes fused with lysosomes (showing red dots); otherwise, it merged with mCherry fluorescence to increase yellow dots, which indicated the autophagosomes that were not fused

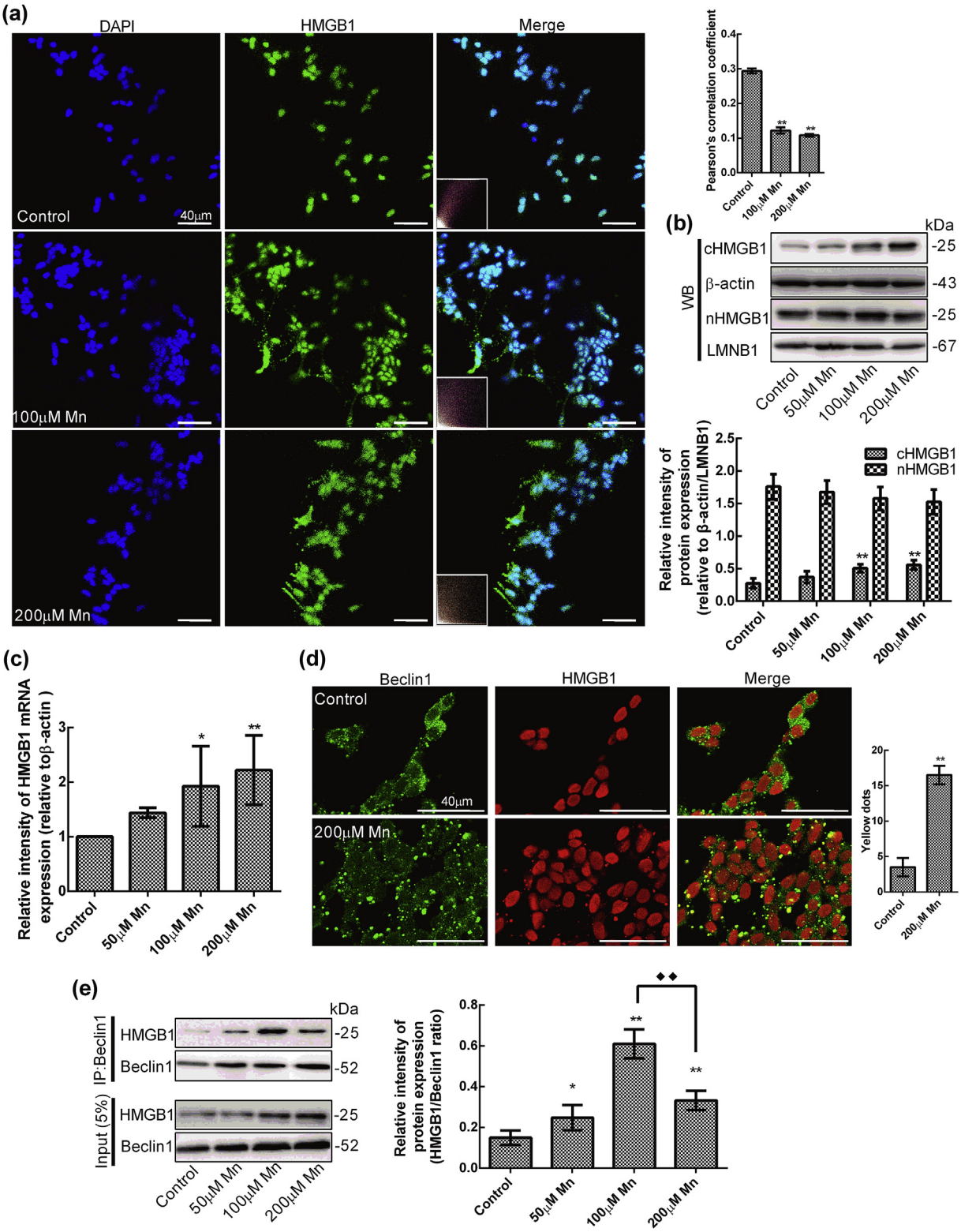

Fig. 1. Mn increased the cytosolic translocation of HMGB1 and HMGB1-Beclin1 binding in SH-SY5Y cells. (a) The translocation of HMGB1 (green) from the nuclei (blue) to cytosol in the control and 100, 200 μM Mn treatments were examined under an Olympus confocal microscope with ×40 magnification and analyzed via calculating the Pearson's correlation coefficient by Image J. An embedded scatter gram in bottom left corner of the merged image estimates the amount of each detected antigens based on colocalization. (b) The expression level of HMGB1 in the cytosolic (cHMGB1) and nuclear (nHMGB1) fraction were determined by western blotting in the control and Mn treatments. β-Actin and LMNB1 were used as loading controls for the cytoplasmic and nuclear fractions, respectively. (c) The HMGB1 mRNA level in the control and Mn treatments was detected by real-time PCR. Relative intensity was normalized to that of β-actin. (d) The colocalization of HMGB1 (red) and Beclin1 (green) in the control and 200 μM Mn treatment was observed under an Olympus confocal microscope with ×40 magnification and analyzed via calculating the amount of yellow dots per 10 cells by Image J. (e) The immunoprecipitation products and semi-quantitative analysis of HMGB1 and Beclin1 in the cytosolic fraction of the control and Mn treatments are shown. The cytosolic lysates were precipitated with anti-Beclin1 antibody. The levels of indicated proteins were analyzed with western blotting. Data are presented as the mean ± SD of three replicates in a representative experiment. $^{*}p < 0.05$ and $^{**}p < 0.01$ vs. control; ◆◆ $p < 0.01$ 200 μM Mn vs. 100 μM Mn treatment. (For interpretation of the references to color in this figure legend, the reader is referred to the Web version of this

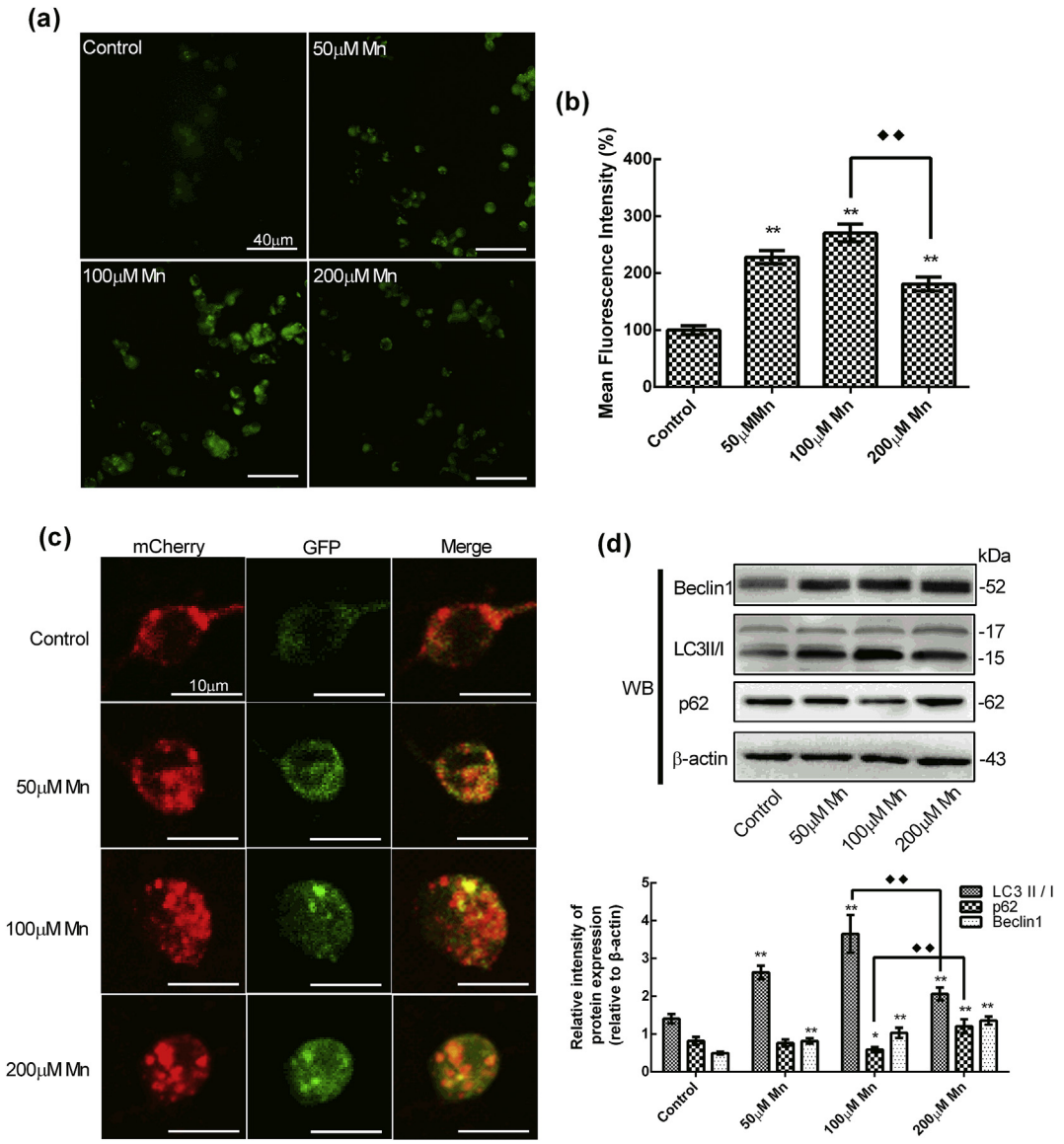

Fig. 2. Mn activated autophagy in SH-SY5Y cells. (a) Autophagic vacuoles labeled by MDC were observed under an inverted fluorescence microscope with ×40 magnification in the control and Mn treatment groups. (b) Flow cytometry determined the fluorescence intensity of autophagic vacuoles labeled by MDC in the control and Mn treatment groups. (c) Representative images of SH-SY5Y cells transfected with Ad-mCherry-GFP-LC3B adenovirus in the control and Mn treatments (Olympus confocal microscope with ×60 magnification). (d) The expression levels of Beclin1, LC3II/I, and p62 were determined by western blotting in the control and Mn treatment groups. Relative intensity was normalized to that of β-actin. Data are presented as the mean ± SD of three replicates in a representative experiment. $^{**}p < 0.01$ vs. control; $^{◆◆}p < 0.01$ 200 μM Mn vs. 100 μM Mn treatment.

with lysosome. The increase of both red and yellow dots indicated the autophagic activation, and yet the increase of yellow dots alone reflected the block of autophagic flux. As shown in Fig. 2c and Supplemental Fig. S1a, there was an obvious increase of both red and yellow dots in the 100 μM Mn treatment; whereas, in the 200 μM Mn treatment, only the increase of yellow dots was observed. Subsequently, the changes of autophagy associated with protein expression (Beclin1, LC3II/I, and p62) were confirmed by western blot. Our results showed that an increase of LC3II/I, an essential component of autophagic membrane structures, an increase of Beclin1, an indispensable protein for autophagy induction, and a decrease of p62, functioning as a receptor for autophagic substrates, were induced by 50 and 100 μM Mn treatment (Fig. 2d). In contrast, a significant decrease of LC3II/I and increase of p62 was present in the 200 μM Mn treatment when compared to 100 μM Mn treatment (Fig. 2d), suggesting an autophagic dysregulation transforming from activation to inhibition. To sum up, the above results further corroborate that Mn induced autophagic dysregulation in SH-SY5Y cells is related to weakened the HMGB1-Beclin1 binding.

3.2. Mn-induced alpha-synuclein overexpression interfered with the interaction of HMGB1 and Beclin1, to subsequently promote Beclin1 binding to Bcl2

As reported previously, Mn exposure could induce nerve-cell apoptosis and α-SYN overexpression, exerting neurotoxicity (Peres et al., 2016), which was consistent with our current data (Fig. 3a and b). As expected, Mn treatment dramatically caused apoptosis and increased the α-SYN expression, as compared to the control (Fig. 3a and b). Of note, there was a significant difference in α-SYN expression between the 100 μM Mn treatment and the 200 μM Mn treatment (Fig. 3b). To explore whether α-SYN was involved in HMGB1-dependent autophagy, we examined the interaction of α-SYN and HMGB1 in the cytosolic fraction of SH-SY5Y cells by immunofluorescence and Co-

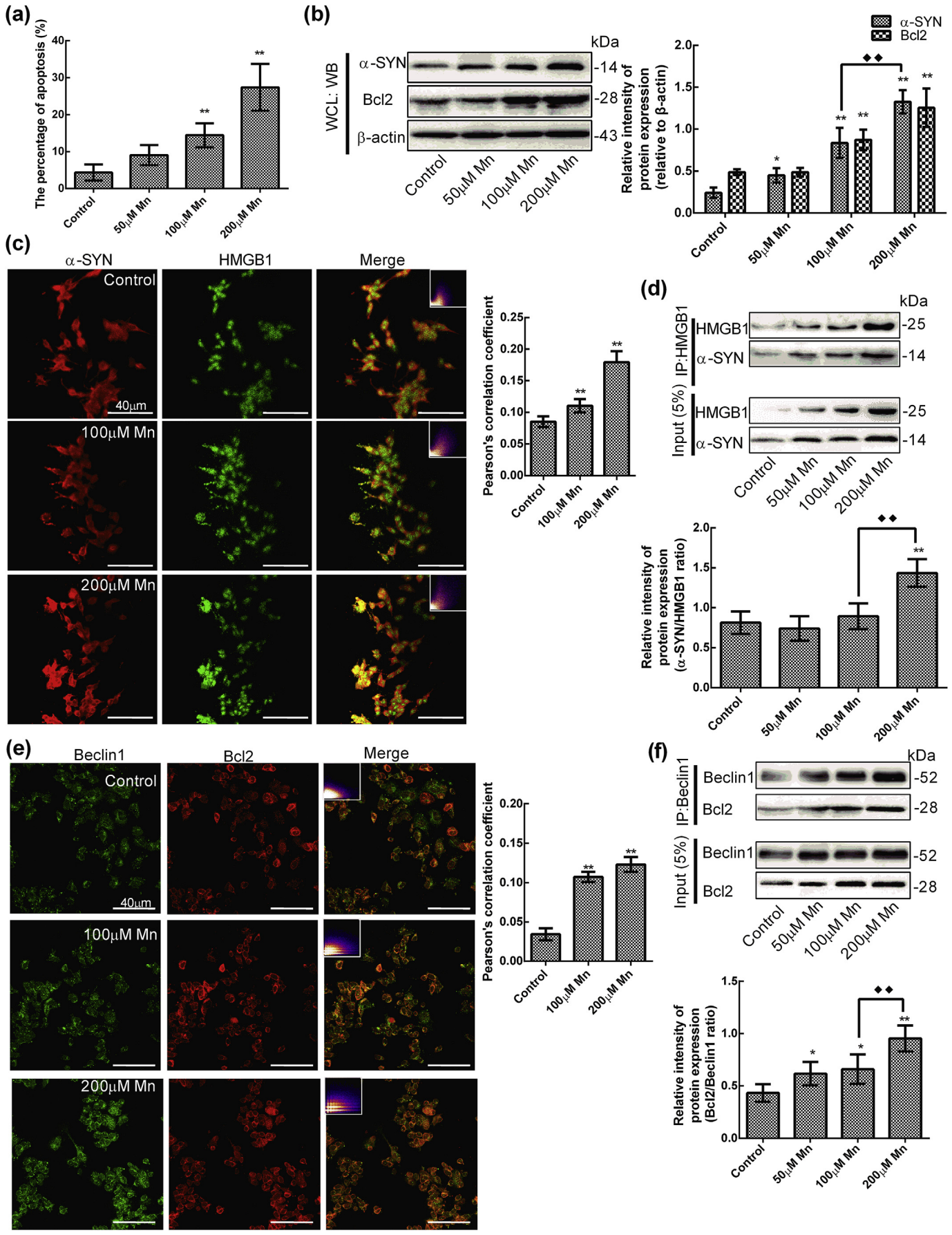

(caption on next page)

Fig. 3. Mn increased the interaction of HMGB1 and α-SYN and the interaction of Beclin1 and Bcl2. (a) The apoptosis in the control and Mn treatments was analyzed by flow cytometry. (b) SH-SY5Y cells were treated with Mn as indicated. The expression levels of α-SYN and Bcl2 in the whole cell lysates were determined by western blotting. Relative intensity was normalized to that of β-actin. (c, e) The colocalization of α-SYN (red) and HMGB1 (green), and Bcl2 (red) and Beclin1 (green) in the control and 100 and 200 μM Mn treatments was observed under an Olympus confocal microscope with ×40 magnification and analyzed via calculating the Pearson's correlation coefficient by Image J. An embedded scatter gram in upper right or left corner of the merged image estimates the amount of each detected antigens based on colocalization. Colocalized pixels of yellow color were located along the diagonal of scatter gram. (d, f) The immunoprecipitation products and semi-quantitative analysis of HMGB1 and α-SYN, and Beclin1 and Bcl2 in the cytosolic fraction of the control and Mn treatments are shown. Cytosolic HMGB1 or Beclin1 were immunoprecipitated. Immunoprecipitates were analyzed by immunoblotting for HMGB1 and α-SYN, or Beclin1 and Bcl2. Data are presented as the mean ± SD of three replicates in a representative experiment. $^{*}p < 0.05$ and $^{**}p < 0.01$ vs. control; ◆◆ $p < 0.01$ 200 μM Mn vs. 100 μM Mn treatment. (For interpretation of the references to color in this figure legend, the reader is referred to the Web version of this article.)

IP assays. As shown in Fig. 3c, the overlay images showed that the remarkable increase in Pearson's correlation coefficient that reflected the colocalization of HMGB1 and α-SYN (merged by α-SYN-Cy3 and HMGB1-FITC) correlated with Mn (100 and 200 μM) treatment. We further confirmed that 200 μM Mn treatment led to a significant increase of α-SYN-HMGB1 binding when compared to 100 μM Mn treatment ($p < 0.05$, Fig. 3d). These results indicated that the inhibition of autophagy by Mn might be due to α-SYN binding to HMGB1 limiting the HMGB1-Beclin1 binding.

In the context of cellular stress, there is a close association between apoptosis and autophagy (Booth et al., 2014). To find the relationship between Mn-induced autophagic dysregulation and apoptosis, we determined Bcl2 expression level in response to Mn treatment. Bcl2 expression significantly increased after Mn (100 and 200 μM) treatment; yet, this increase failed to resist Mn-induced apoptosis (Fig. 3a and b). Subsequently, we measured the interaction of Beclin1 and Bcl2 in the cytosolic fraction of SH-SY5Y cells. We demonstrated that Mn treatment significantly enhanced the interaction of Beclin1 and Bcl2, which was supported by immunofluorescence and Co-IP assays, showing increased intensity and colocalization of Beclin1-FITC and Bcl2-Cy3 upon Mn exposure (Fig. 3e and f). Interestingly, Beclin1-Bcl2 binding was more greatly increased in 200 μM Mn treatment than that in 100 μM Mn treatment. These results suggested that the inhibition of autophagy by Mn could exacerbate apoptosis via promoting Beclin1 binding to Bcl2.

3.3. Cory B ameliorated the autophagic inhibition and neurotoxicity induced by Mn

As previously discovered, Cory B is identified as a new autophagy inducer (Chen et al., 2014). In this study, we used different concentrations of Cory B (25–100 μM) pretreatment to assess whether Cory B could relieve Mn-induced autophagic inhibition in SH-SY5Y cells. The levels of LDH release and CCK8 as well as apoptosis reflected obvious neurotoxicity in 200 μM Mn-treated SH-SY5Y cells and a non-toxic effect in the 100 μM Cory B-alone treated group (Fig. 4a and b). In comparison with 200 μM Mn treatment, the neurotoxicity was accompanied by an obvious remission in 100 μM Cory B pretreatment (Fig. 4a and b). Additionally, 100 μM Cory B pretreatment potently enhanced the MDC-labeled positive autophagy vesicles compared to 200 μM Mn treatment (Fig. 4c and d). As autophagy is a dynamic process, further research using Ad-mCherry-GFP-LC3B adenovirus and western blotting assay confirmed that pretreatment with 100 μM Cory B significantly facilitated autophagy flux, as shown by increase of both red and yellow dots in merged images, substantial increase of LC3II/I, and significant decrease of p62 expression, compared to 200 μM Mn treatment (Fig. 4e and f, Supplemental Fig. S1b). In other words, these data suggested that Cory B could ameliorate the inhibition of autophagy and apoptosis induced by Mn.

3.4. Cory B strengthened HMGB1-Beclin1 binding via dissociating HMGB1 from alpha-synuclein to subsequently inhibit Beclin1-Bcl2 binding upon Mn exposure

To figure out how Cory B ameliorated the inhibition of autophagy and neurotoxicity in 200 μM Mn-treated SH-SY5Y cells, we carried out a series of experiments to examine the possible molecular mechanism. Western blot analysis showed there were no obvious effect on the expression of α-SYN and Bcl2 in Cory B (25–100 μM) pretreatment when compared to 200 μM Mn treatment (Fig. 5a). Based on our findings on Mn-induced autophagic dysregulation, we detected the interactions of HMGB1 and α-SYN, HMGB1 and Beclin1, and Beclin1 and Bcl2 in the cytosolic fraction of SH-SY5Y cells, respectively, after Cory B pretreatment. The merged images by laser confocal microscopy and Co-IP assay revealed that 100 μM Cory B pretreatment strongly reduced the colocalization and interaction of HMGB1 and α-SYN compared to 200 μM Mn treatment (Fig. 5a and b). In contrast, a significant increase of HMGB1 and Beclin1 binding was caused by 100 μM Cory B pretreatment compared to 200 μM Mn treatment, evidenced by immunofluorescence and Co-IP assays (Fig. 6a and c). Accordingly, the results of Fig. 6b and c revealed a significant reduction of Beclin1-Bcl2 binding in 100 μM Cory B pretreatment when compared to 200 μM Mn treatment. These above results suggested that Cory B strengthened the HMGB1-Beclin1 binding via dissociating HMGB1 from α-SYN.

3.5. Cory B ameliorated Mn-induced the inhibition of autophagy through inhibiting the mTOR pathway

Mammalian target of rapamycin (mTOR) has been identified as a major negative regulator of mammalian autophagy and is thought to be involved in the regulation of various biological functions (Karlsson et al., 2013). To explore the potential mechanism of Cory B in Mn-induced autophagic inhibition, we investigated mTOR signaling in response to Mn treatment, Cory B-alone treatment, and Cory B pretreatment. 4E-binding protein 1 (4EBP1) and the p70 ribosomal S6 kinases (S6K1), as downstream effectors of mTOR signaling, reflect mTOR activity. We found that 100 μM Cory B-alone and 100 and 200 μM Mn treatments could potently inhibit the mTOR pathway, as evidenced by the ratio of phospho-mTOR to total mTOR, the ratio of phospho-4EBP1 to total 4EBP1, and the ratio of phospho-S6K1 to total S6K1 reduction (Fig. 7a and b). Moreover, 100 μM Cory B pretreatment further strongly suppressed mTOR in Mn-induced autophagic inhibition (Fig. 7b). These data indicated that inhibition of mTOR signaling by Cory B might be another potential mechanism in ameliorating Mn-induced inhibition of autophagy.

4. Discussion

In the current study, we demonstrated that Mn overexposure stimulated nucleus-to-cytosol translocation of HMGB1, restricted cytosolic HMGB1-dependent autophagic induction because of α-SYN overexpression, and thus exacerbated apoptosis induced by Beclin1-Bcl2 binding increase. Moreover, we found the neuroprotective role of Cory B in Mn-induced inhibition of autophagy and apoptosis could be partly attributed to dissociating HMGB1 from α-SYN and inhibiting mTOR signaling (Fig. 8).

HMGB1 plays important nuclear, cytosolic, and extracellular roles in the regulation of autophagy during various stress conditions (e.g., inflammation, trauma, oxidative, and metabolic stress) (Kang et al., 2010; Sun and Tang, 2014). Cytosolic HMGB1-Beclin1 binding is an important event for autophagic induction (Sun and Tang, 2014).

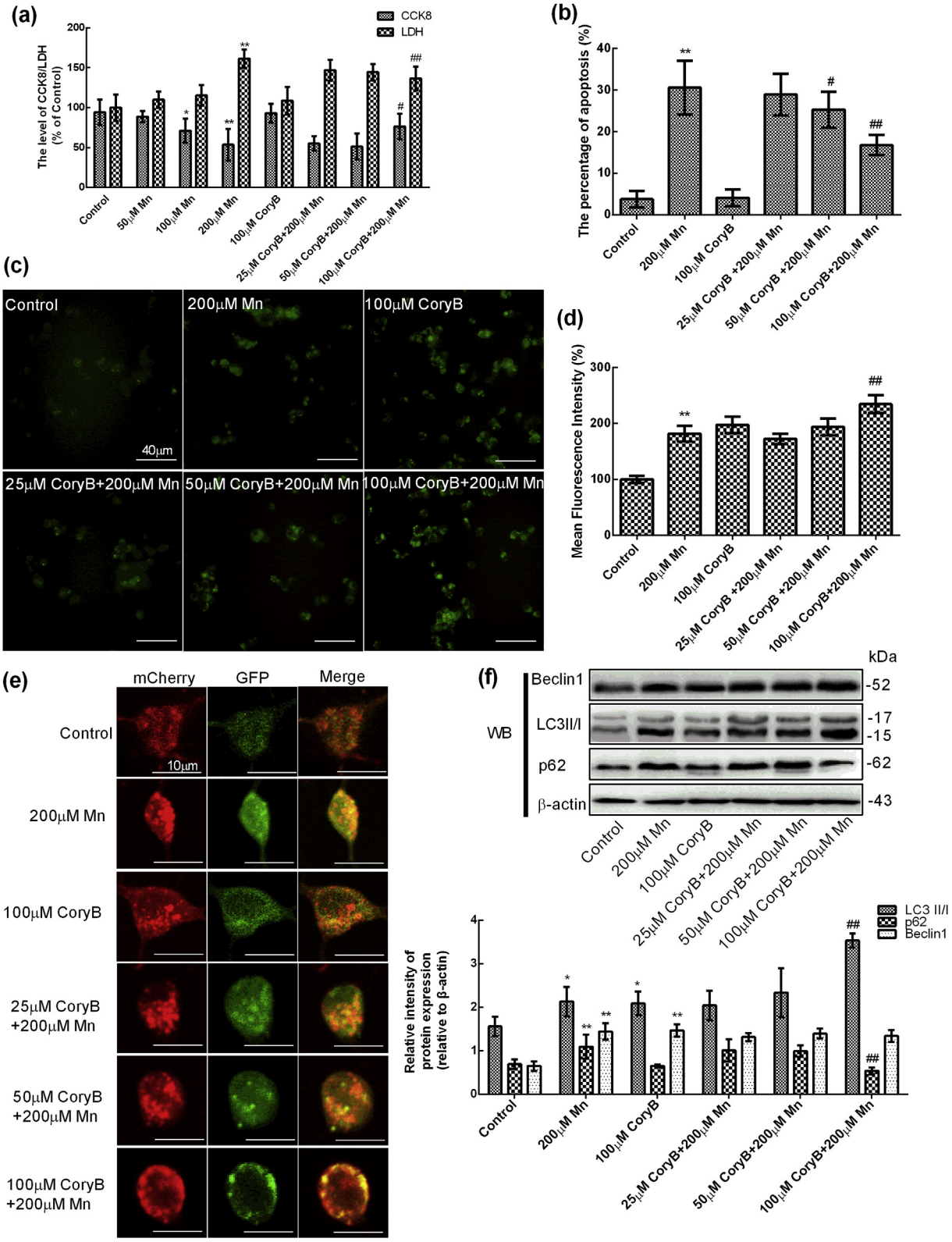

Fig. 4. Cory B ameliorated Mn-induced autophagic inhibition and neurotoxicity. (a) Cell damage and viability were determined by measuring LDH and CCK8 levels using commercial kits in the control, Mn treatment, and Cory B pretreatment groups. (b) Flow cytometry detected apoptosis in the control, 200 μM Mn treatment, and Cory B pretreatment groups. (c) Autophagic vacuoles labeled by MDC were observed under an inverted fluorescence microscope with ×40 magnification in the control, 200 μM Mn treatment, and Cory B pretreatment groups. (d) Flow cytometry determined the fluorescence intensity of autophagic vacuoles labeled by MDC in the control, 200 μM Mn treatment, and Cory B pretreatment groups (e) Representative images of SH-SY5Y cells transfected with Ad-mCherry-GFP-LC3B adenovirus in the control, 200 μM Mn treatment, and Cory B pretreatment groups (Olympus confocal microscope with ×60 magnification). (f) The expression levels of Beclin1, LC3II/I, and p62 were determined by western blotting in the control, 200 μM Mn treatment, and Cory B pretreatment groups. Relative intensity was normalized to that of β-actin. Data are presented as the mean ± SD of three replicates in a representative experiment. $^{*}p < 0.05$ and $^{**}p < 0.01$ vs. control; $^{\#}p < 0.05$ and $^{\#\#}p < 0.01$ vs. 200 μM Mn treatment.

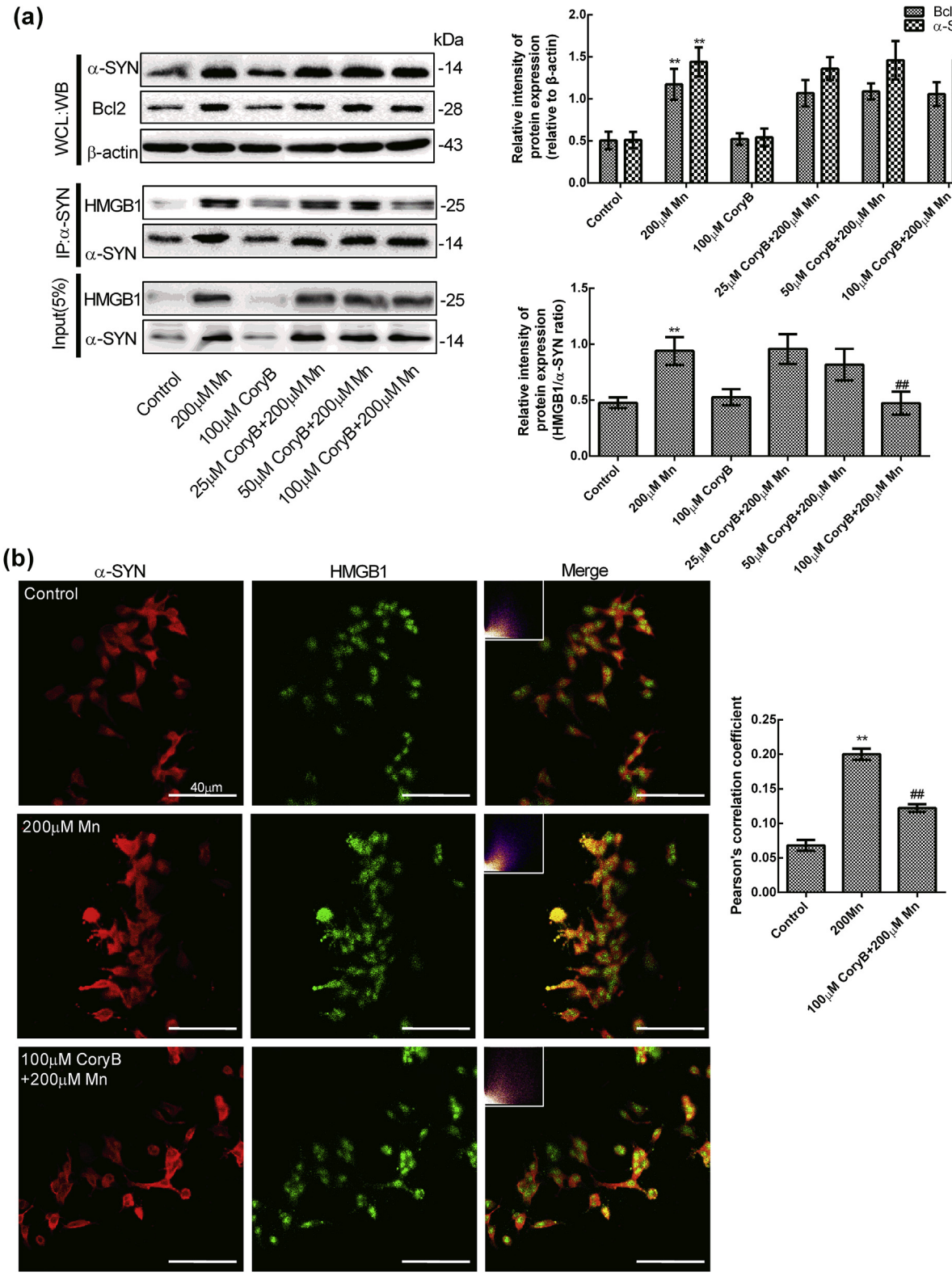

Fig. 5. Cory B weakened the interaction of HMGB1 and α-SYN. (a) SH-SY5Y cells were pretreated with Cory B as indicated. Expression levels of α-SYN and Bcl2 in the whole-cell lysates were determined by western blotting. Relative intensity was normalized to that of β-actin. The immunoprecipitation products and semi-quantitative analysis of HMGB1 and α-SYN are also shown. Cytosolic α-SYN were immunoprecipitated. Immunoprecipitates were analyzed by immunoblotting for HMGB1 and α-SYN. (b) The colocalization of α-SYN (red) and HMGB1 (green) in the control, 200 μM Mn treatment, and 100 μM Cory B pretreatment groups was observed under an Olympus confocal microscope with ×40 magnification and analyzed via calculating the Pearson's correlation coefficient by Image J. An embedded scatter gram in upper left corner of the merged image estimates the amount of each detected antigens based on colocalization. Colocalized pixels of yellow color were located along the diagonal of scatter gram. Data are presented as the mean ± SD of three replicates in a representative experiment. $^{*}p < 0.05$ and $^{**}p < 0.01$ vs. control; $^{\#\#}p < 0.01$ vs. 200 μM Mn treatment. (For interpretation of the references to color in this figure legend, the reader is referred to the Web version of this article.)

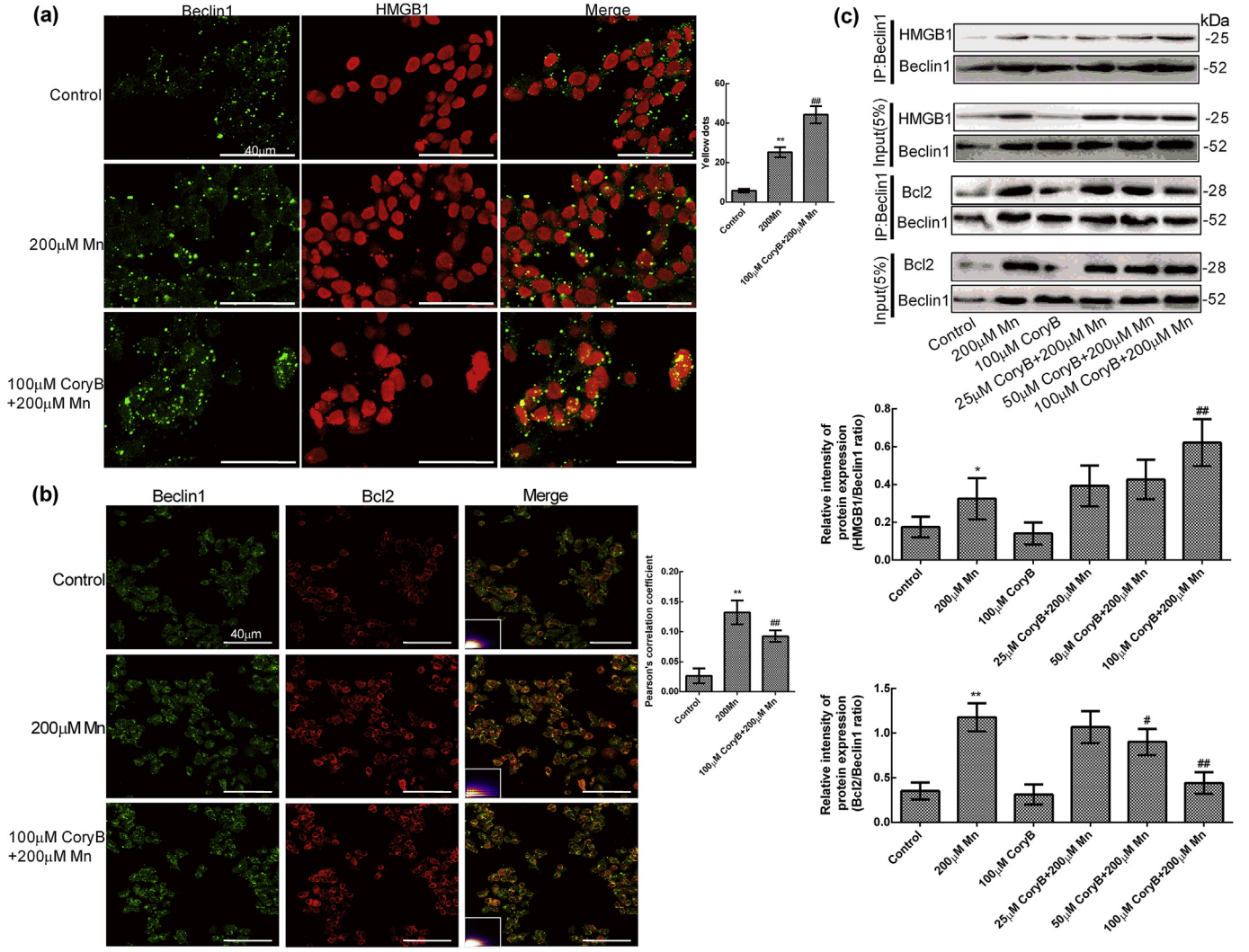

Fig. 6. Cory B increased the interaction of HMGB1 and Beclin1, resulting in the dissociation of Beclin1 from Bcl2. (a, b) The colocalization of HMGB1 (red) and Beclin1 (green), and Bcl2 (red) and Beclin1 (green) in the control, 200 μM Mn treatment, and 100 μM Cory B pretreatment groups was observed under an Olympus confocal microscope with × 40 magnification and analyzed via calculating the amount of yellow dots per 10 cells or Pearson's correlation coefficient by Image J. An embedded scatter gram in bottom left corner of the merged image estimates the amount of each detected antigens based on colocalization. Colocalized pixels of yellow color were located along the diagonal of scatter gram. (c) The immunoprecipitation products and semi-quantitative analysis of HMGB1 and Beclin1, and Beclin1 and Bcl2 in the cytosolic fraction of the control and Mn treatments are shown. Cytosolic Beclin1 were immunoprecipitated. Immunoprecipitates were analyzed by immunoblotting for HMGB1 and Beclin1, or Beclin1 and Bcl2. Data are presented as the mean ± SD of three replicates in a representative experiment. $^{*}p < 0.05$ and $^{**}p < 0.01$ vs. control; $^{\#}p < 0.05$ and $^{\#\#}p < 0.01$ vs. 200 μM Mn treatment. (For interpretation of the references to color in this figure legend, the reader is referred to the Web version of this article.)

HMGB1, as a novel regulator between autophagy and apoptosis, is involved in several neurodegenerative disorders such as PD, amyotrophic lateral sclerosis, Alzheimer's disease (AD), and Huntington's disease (HD) (Zhu et al., 2015). Structurally, the intramolecular disulfide bridge (C23/45) of HMGB1 is able to bind Beclin1 to regulate autophagy, and subsequently lead to the dissociation of Bcl2 from Beclin1 to promote cell survival (Kang et al., 2010, 2011). In this study, injury to SH-SY5Y cells was assessed by measuring LDH and CCK8 levels. Different doses of Mn (50–200 μM) progressively induced nerve cell damage and provided an ideal condition for further investigation. Our first observation was that Mn (100, 200 μM) treatment could obviously increase the HMGB1 mRNA level, stimulate cytosolic translocation of HMGB1, and increase the cytosolic HMGB1-Beclin1 binding, whereas in 200 μM Mn-treated SH-SY5Y cells, this binding was extremely decreased. Next, we carried out a series of experiments to assess autophagy. Our data showed that Mn activated basal autophagy supported by enhancing MDC-labeled autophagic vesicles, the changes of autophagy flux, and the expression of Beclin1 and LC3II/I. However, autophagic inhibition occurred in 200 μM Mn treatment accompanied by a decrease of cytosolic HMGB1-Beclin1 binding, the accumulation of p62, and the block of autophagy flux, when compared to 100 μM Mn treatment. These data indicated that Mn exposure could activate basal autophagy and promote the initiation but not sustaining of autophagy. Therefore, we speculated that Mn has an effect on autophagy by interfering with the interaction of HMGB1 and Beclin1.

The regulation of autophagy was controlled by multiple protein complexes (HMGB1/p53, HMGB1-HSPB1, Beclin1-VPS34-Atg14L) (Livesey et al., 2012; Sun and Tang, 2014; Huang et al., 2017). Beclin1 plays an essential role in autophagic initiation by interacting with various cofactors (Atg14L, UVRAG, Bif-1, Vsp34, and HMGB1) (Kang et al., 2011). So, HMGB1-Beclin1 is one of the most regulators for autophagic induction. HMGB1 confers pro-autophagic activities, likely by controlling Beclin1–Bcl-2 complex formation. The dissociation of Bcl-2 from Beclin1 is an important mechanism involved in activating autophagy and limiting apoptosis in response to starvation and potentially after other physiological stimuli (Pattingre et al., 2005). HMGB1

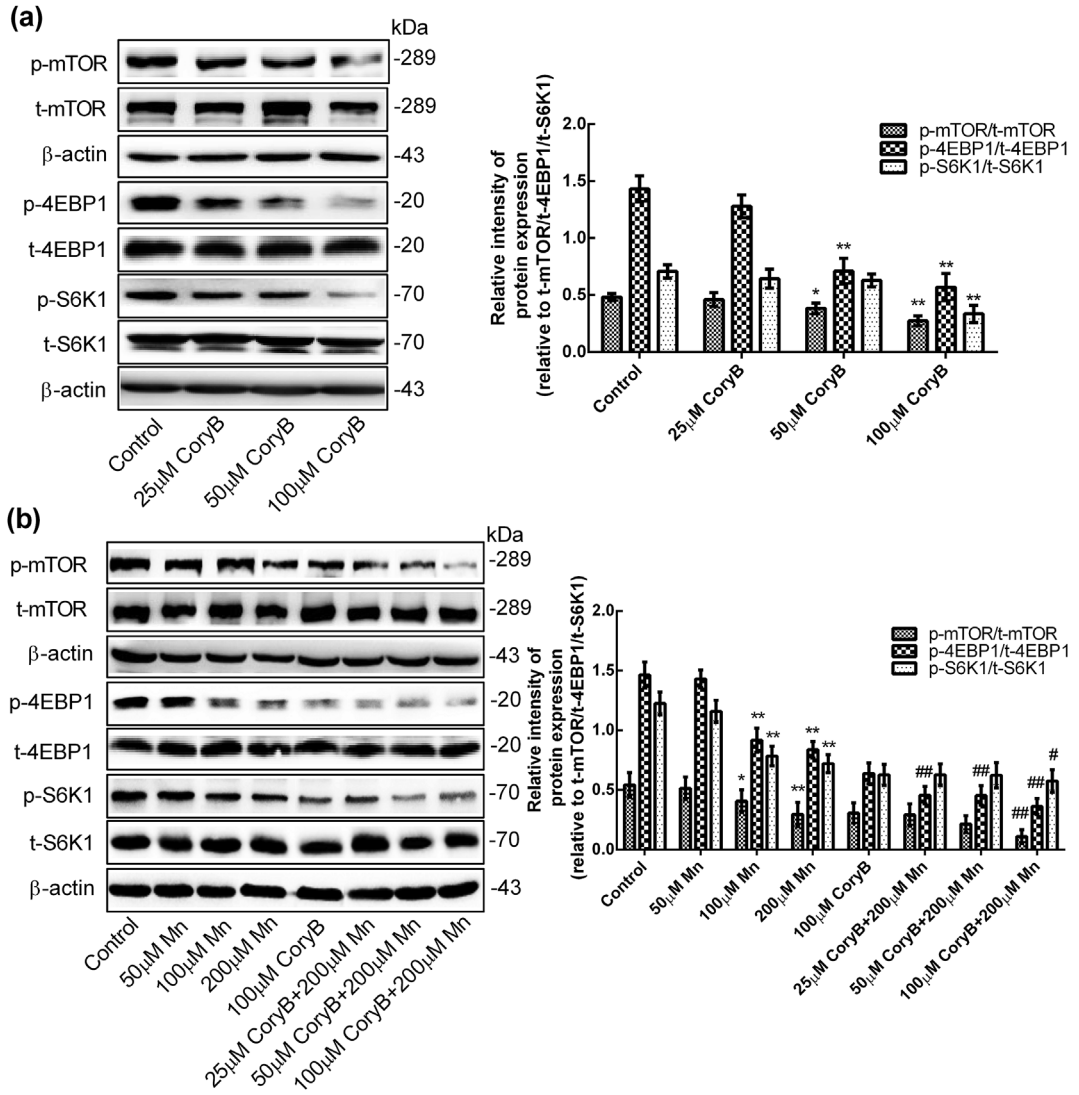

Fig. 7. Cory B inhibited mTOR signaling. (a, b) The expression levels of total mTOR (t-mTOR), p-mTOR, total 4EBP1 (t-4EBP1), p-4EBP1, total S6K1 (t-S6K1), and p-S6K1 in the control, Mn treatment, Cory B treatment, and pretreatment groups were determined by western blotting. Relative intensity was normalized to that of β-actin. Data are presented as the mean ± SD of three replicates in a representative experiment. $^{*}p < 0.05$ and $^{**}p < 0.01$ vs. control; $^{\#}p < 0.05$ and $^{\#\#}p < 0.01$ vs. 200 μM Mn treatment.

recently has been reported to bind preferentially to overexpressed α-SYN, restrict its cytosolic translocation and interact with Beclin1, consequently impairing autophagy (Huang et al., 2017; Song et al., 2014; Wang et al., 2016). Moreover, Beclin1 interacts with anti-apoptotic protein Bcl2 revealing the cross talk between apoptosis and autophagy (Kang et al., 2011). Many studies have reported that Mn can induce α-SYN overexpression and oligomerization, autophagic dysregulation in dose-dependent manner, mitochondrial dysfunction, oxidative stress, etc., of which α-SYN overexpression and oligomerization can further exacerbate neurotoxicity of Mn (O'Neal and Zheng, 2015; Peres et al., 2016). Herein, to understand how Mn interferes with HMGB1-Beclin1 binding, we launched an in-depth investigation. Our results corroborated with previous findings that demonstrated that Mn could induce α-SYN overexpression (Xu et al., 2014a, 2014b, 2015). Additionally, we also found that the increase of Bcl2 expression by Mn did not relieve apoptosis. Meanwhile, in 200 μM Mn-treated SH-SY5Y cells, cytosolic HMGB1-α-SYN binding and cytosolic Beclin1-Bcl2 binding both substantially increased. The significant changes among these protein complexes between 100 μM and 200 μM Mn treatment might be due to the overexpression of α-SYN induced by 200 μM Mn. Peres et al. have reported that at the early stage of Mn exposure, the increase of α-synuclein expression was regarded as a Mn store, appearing to be neuroprotective against Mn-induced neurotoxicity. At later points, α-synuclein continued exposure to Mn promoted α-synuclein overexpression and oligomers, exerting its neurotoxicity (Peres et al., 2016). These results indicated Mn-induced overexpression of α-SYN could lead to inhibition of autophagy via preferentially binding to HMGB1 to block HMGB1-Beclin1 interaction, and ultimately resulting in apoptosis via enhancing the Beclin1-Bcl2 interaction. Besides this, we also cannot rule out that the protein complexes switch among binding partners because of the actions of Mn in part.

Recently, Cory B, a natural autophagy enhancer isolated from Chinese herbal medicine, has been reported to play a neuroprotective role for the treatment of PD (Chen et al., 2014). Moreover, Song et al. revealed that Cory B could restore the deficient cytosolic translocation of HMGB1 and autophagy induced by α-SYN overexpression (Song et al., 2014). Based on these findings, we used 25, 50, and 100 μM Cory B pretreatment to explore the safety and effective dose to ameliorate the inhibition of autophagy by Mn. The release level of LDH and CCK8 suggested that 100 μM Cory B pretreatment could effectively ameliorate Mn-induced cytotoxicity and apoptosis. However, Bcl2 expression showed no changes with Cory B (25–100 μM) pretreatment compared to

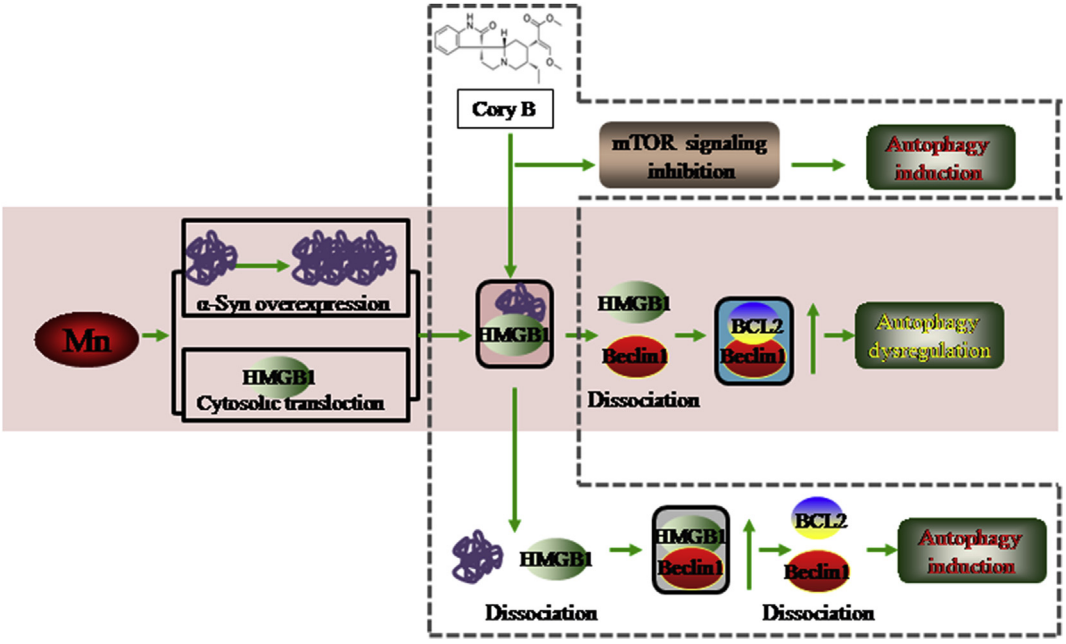

Fig. 8. Possible mechanism of Cory B ameliorating Mn-induced autophagic inhibition by inhibiting HMGB1-α-SYN binding and mTOR signaling. Mn stimulated the cytosolic translocation of HMGB1, causing autophagic dysregulation by overexpression of α-SYN, thereby resulting in apoptosis aggravated by the increase of the Beclin1-Bcl2 binding. Cory B could increase the interaction of HMGB1 and Beclin1 via blocking HMGB1-α-SYN binding, subsequently ameliorating apoptosis by the Beclin1-Bcl2 binding reduction in Mn-induced autophagic dysregulation and neurotoxicity. In addition, Cory B could inhibit mTOR signaling leading to ameliorating Mn-induced autophagic dysregulation.

200 μM Mn treatment, ruling out the effect of Cory B on anti-apoptotic protein Bcl2. Besides, 100 μM Cory B pretreatment had also been evidenced to facilitate the autophagy flux. To explore the reasons, we used laser confocal microscopy and Co-IP to examine the molecular interaction in the cytosolic fractions. We found that 100 μM Cory B pretreatment could weaken the interaction of HMGB1-α-SYN and strengthen HMGB1-Beclin1 binding, resulting in the reduction of Beclin1-Bcl2 binding in the cytosolic fraction compared to 200 μM Mn treatment. These results further corroborated that Cory B could ameliorate the Mn-induced inhibition of autophagy via dissociating cytosolic HMGB1 from α-SYN to bind to Beclin1, and then ameliorate apoptosis via inhibiting Beclin1-Bcl2 binding. However, our data showed no significant change of α-SYN expression in Cory B (25–100 μM) pretreatment when compared to 200 μM Mn treatment, the reason for which might be the lack of sustaining autophagy flux and related with lysosomal dysfunction (Chen et al., 2014; Tang et al., 2010). HMGB1 has been shown to regulate autophagy related with reactive oxygen species (Sun and Tang, 2014). Moreover, lysosomes, as an important site for the degradation of misfolded proteins, are also vulnerable to extracellular stimulus (Chen et al., 2014; Funakoshi et al., 2013; Jackson and Hewitt, 2016). Therefore, more studies on the effect of Mn on redox of HMGB1 and lysosome are required.

Many previous studies have reported that Mn exposure could affect the autophagy process by various pathways, such as the activation of mTOR and p70S6K signaling, induction of apoptotic cascade signaling, α-SYN overexpression, ER stress, and oxidative stress (Liu et al., 2017; Xilouri et al., 2016; Yuan et al, 2016; Zhou et al., 2017). mTOR signaling can impact the onset and progression of neurodegenerative diseases such as PD, HD, epilepsy, stroke, and trauma (Karlsson et al., 2013). In the nervous system, the inhibition of mTOR signaling is involved in the process of autophagic induction and plays neuroprotective role in promoting nerve cell survival (Chen et al., 2014). t-S6K1 and t-4EBP1, as downstream components of mTOR can reflect the activation of mTOR signaling. Our results showed that Mn treatment significantly decreased the ratio of p-mTOR to t-mTOR, the ratio of p-S6K1 to t-S6K1, and the ratio of p-4EBP1 to t-4EBP1, indicating the inhibition of mTOR signaling in the process of Mn-induced autophagy. A similar result of mTOR inhibition was also observed in 100 μM Cory B-alone treatment, further verifying its positive effect on autophagy. Furthermore, 100 μM Cory B pretreatment strongly inhibited mTOR signaling in the process of Mn-induced autophagic inhibition. These results clearly implied that Cory B restored inhibition of autophagy via further promoting inhibition of the mTOR pathway to some extent, in addition to interfering with HMGB1-α-SYN interaction.

5. Conclusions

The results of the present study revealed the effect of Mn on cytosolic HMGB1-dependent autophagy. Besides, we have also confirmed the neuroprotective role of Cory B in restoring the deficiency of autophagy to promote nerve cell survival, via dissociating HMGB1 from overexpressed α-SYN and inhibiting mTOR signaling. Further studies will be required to not only understand HMGB1 and its multifunctional effects but also explore the lysosomal function in the setting of Mn-induced neurotoxicity.

Author contributions

DYY cultured SH-SY5Y cells and detected relative indicators, including LDH release level and CCK8 level, immunofluorescence and co-IP assays, western blot assay, as well as analysis, writing of the manuscript and figure artwork. CL and ZM performed apoptosis and MDC staining assays by flow cytometry. CW performed PCR analysis. YD and WL guided experimental operation. BX performed experimental design and modification of the manuscript. All authors revised the article critically for intellectual content and have read and approved the final version of the manuscript.

Funding

This work was supported by National Natural Science Foundation of China (81773377).

Compliance with ethical standards

Not applicable.

Conflicts of interest

The authors declare that they have no competing interests.

Acknowledgements

Not applicable.

Transparency document

Transparency document related to this article can be found online at https://doi.org/10.1016/j.fct.2018.12.027.

Appendix A. Supplementary data

Supplementary data to this article can be found online at https://doi.org/10.1016/j.fct.2018.12.027.

References

Booth, L.A., Tavallai, S., Hamed, H.A., Cruickshanks, N., Dent, P., 2014. The role of cell signalling in the crosstalk between autophagy and apoptosis. Cell. Signal. 26, 549–555.
Chen, L.L., Song, J.X., Lu, J.H., Yuan, Z.W., Liu, L.F., Durairajan, S.S., Li, M., 2014. Corynoxine, a natural autophagy enhancer, promotes the clearance of alpha-synuclein via Akt/mTOR pathway. J. Neuroimmune Pharmacol. 9, 380–387.
Chen, P., Chakraborty, S., Mukhopadhyay, S., Lee, E., Paoliello, M.M., Bowman, A.B., Aschner, M., 2015. Manganese homeostasis in the nervous system. J. Neurochem. 134, 601–610.
Funakoshi, T., Aki, T., Unuma, K., Uemura, K., 2013. Lysosome vacuolation disrupts the completion of autophagy during norephedrine exposure in SH-SY5Y human neuroblastoma cells. Brain Res. 1490, 9–22.
Huang, J., Yang, J., Shen, Y., Jiang, H., Han, C., Zhang, G., Liu, L., Xu, X., Li, J., Lin, Z., Xiong, N., Zhang, Z., Xiong, J., Wang, T., 2017. HMGB1 mediates autophagy dysfunction via perturbing beclin1-vps34 complex in dopaminergic cell model. Front. Mol. Neurosci. 10, 13.
Jackson, M.P., Hewitt, E.W., 2016. Cellular proteostasis: degradation of misfolded proteins by lysosomes. Essays Biochem. 60, 173–180.
Jin, M., Klionsky, D.J., 2014. Regulation of autophagy: modulation of the size and number of autophagosomes. FEBS Lett. 588, 2457–2463.
Kang, R., Livesey, K.M., Zeh, H.J., Loze, M.T., Tang, D., 2010. HMGB1: a novel Beclin 1-binding protein active in autophagy. Autophagy 6, 1209–1211.
Kang, R., Zeh, H.J., Lotze, M.T., Tang, D., 2011. The Beclin 1 network regulates autophagy and apoptosis. Cell Death Differ. 18, 571–580.
Karlsson, E., Perez-Tenorio, G., Amin, R., Bostner, J., Skoog, L., Fornander, T., Sgroi, D.C., Nordenskjold, B., Hallbeck, A.L., Stal, O., 2013. The mTOR effectors 4EBP1 and S6K2 are frequently coexpressed, and associated with a poor prognosis and endocrine resistance in breast cancer: a retrospective study including patients from the randomised Stockholm tamoxifen trials. Breast Cancer Res. 15, R96.
Liu, C., Yan, D.Y., Tan, X., Ma, Z., Wang, C., Deng, Y., Liu, W., Yang, T.Y., Xu, Z.F., Xu, B., 2017. Effect of the cross-talk between autophagy and endoplasmic reticulum stress on Mn-induced alpha-synuclein oligomerization. Environ. Toxicol. 315–324.
Livesey, K.M., Kang, R., Vernon, P., Buchser, W., Loughran, P., Watkins, S.C., Zhang, L., Manfredi, J.J., Zeh, H.J., Li, L., Lotze, M.T., Tang, D., 2012. p53/HMGB1 complexes regulate autophagy and apoptosis. Cancer Res. 8, 1996–2005.
Lynch-Day, M.A., Mao, K., Wang, K., Zhao, M., Klionsky, D.J., 2012. The role of autophagy in Parkinson's disease. Cold Spring Harb. Perspect. Med. 2, a009357.
Murrow, L., Debnath, J., 2013. Autophagy as a stress-response and quality-control mechanism: implications for cell injury and human disease. Annu. Rev. Pathol. 8, 105–137.
O'Neal, S.L., Zheng, W., 2015. Manganese toxicity upon overexposure: a decade in review. Curr. Environ. Health Rep. 2, 315–328.
Peres, T.V., Parmalee, N.L., Martinez-Finley, E.J., Aschner, M., 2016. Untangling the manganese-alpha-synuclein web. Front. Neurosci. 10, 364.
Pattingre, S., Tassa, A., Qu, X., Garuti, R., Liang, X.H., Mizushima, N., Packer, M., Schneider, M.D., Levine, B., 2005. Bcl-2 antiapoptotic proteins inhibit Beclin 1-dependent autophagy. Cell 6, 927–939.
Ravanan, P., Srikumar, I.F., Talwar, P., 2017. Autophagy: the spotlight for cellular stress responses. Life Sci. 53–67.
Song, J.X., Lu, J.H., Liu, L.F., Chen, L.L., Durairajan, S.S., Yue, Z., Zhang, H.Q., Li, M., 2014. HMGB1 is involved in autophagy inhibition caused by SNCA/alpha-synuclein overexpression: a process modulated by the natural autophagy inducer corynoxine B. Autophagy 10, 144–154.
Sun, X., Tang, D., 2014. HMGB1-dependent and -independent autophagy. Autophagy 10, 1873–1876.
Tang, D., Kang, R., Livesey, K.M., Cheh, C.W., Farkas, A., Loughran, P., Hoppe, G., Bianchi, M.E., Tracey, K.J., Zeh, H.J., Lotze, M.T., 2010. Endogenous HMGB1 regulates autophagy. J. Cell Biol. 190, 881–892.
Tang, D., Kang, R., Zeh, H.J., Lotze, M.T., 2011. High-mobility group box 1, oxidative stress, and disease. Antioxidants Redox Signal. 14, 1315–1335.
Wang, K., Huang, J., Xie, W., Huang, L., Zhong, C., Chen, Z., 2016. Beclin1 and HMGB1 ameliorate the alpha-synuclein-mediated autophagy inhibition in PC12 cells. Diagn. Pathol. 11, 15.
Wirawan, E., Lippens, S., Vanden Berghe, T., Romagnoli, A., Fimia, G.M., Piacentini, M., Vandenabeele, P., 2012. Beclin1: a role in membrane dynamics and beyond. Autophagy 8, 6–17.
Xilouri, M., Brekk, O.R., Stefanis, L., 2016. Autophagy and alpha-synuclein: relevance to Parkinson's disease and related synucleopathies. Mov. Disord. 31, 178–192.
Xu, B., Jin, C.H., Deng, Y., Liu, W., Yang, T.Y., Feng, S., Xu, Z.F., 2014a. Alpha-synuclein oligomerization in manganese-induced nerve cell injury in brain slices: a role of NO-mediated S-nitrosylation of protein disulfide isomerase. Mol. Neurobiol. 50, 1098–1110.
Xu, B., Liu, W., Deng, Y., Yang, T.Y., Feng, S., Xu, Z.F., 2015. Inhibition of calpain prevents manganese-induced cell injury and alpha-synuclein oligomerization in organotypic brain slice cultures. PLoS One 10, e0119205.
Xu, B., Wang, F., Wu, S.W., Deng, Y., Liu, W., Feng, S., Yang, T.Y., Xu, Z.F., 2014b. alpha-Synuclein is involved in manganese-induced ER stress via PERK signal pathway in organotypic brain slice cultures. Mol. Neurobiol. 49, 399–412.
Xu, B., Wu, S.W., Lu, C.W., Deng, Y., Liu, W., Wei, Y.G., Yang, T.Y., Xu, Z.F., 2013. Oxidative stress involvement in manganese-induced alpha-synuclein oligomerization in organotypic brain slice cultures. Toxicology 305, 71–78.
Yu, Y., Tang, D., Kang, R., 2015. Oxidative stress-mediated HMGB1 biology. Front. Physiol. 6, 93.
Yuan, Z., Ying, X.P., Zhong, W.J., Tian, S.M., Wang, Y., Jia, Y.R., Chen, W., Fu, J.L., Zhao, P., Zhou, Z.C., 2016. Autophagy attenuates MnCl2-induced apoptosis in human bronchial epithelial cells. Biomed. Environ. Sci. 29, 494–504.
Zhang, J., Cao, R., Cai, T., Aschner, M., Zhao, F., Yao, T., Chen, Y., Cao, Z., Luo, W., Chen, J., 2013. The role of autophagy dysregulation in manganese-induced dopaminergic neurodegeneration. Neurotox. Res. 24, 478–490.
Zhang, Z., Miah, M., Culbreth, M., Aschner, M., 2016. Autophagy in neurodegenerative diseases and metal neurotoxicity. Neurochem. Res. 41, 409–422.
Zhou, Q., Fu, X., Wang, X., Wu, Q., Lu, Y., Shi, J., Klaunig, J.E., Zhou, S., 2017. Autophagy plays a protective role in Mn-induced toxicity in PC12 cells. Toxicology 394, 45–53.
Zhu, X., Messer, J.S., Wang, Y., Lin, F., Cham, C.M., Chang, J., Billiar, T.R., Lotze, M.T., Boone, D.L., Chang, E.B., 2015. Cytosolic HMGB1 controls the cellular autophagy/apoptosis checkpoint during inflammation. J. Clin. Invest. 125, 1098–1110.
Zinchuk, V., Zinchuk, O., Okada, T., 2007. Quantitative colocalization analysis of multicolor confocal immunofluorescence microscopy images: pushing pixels to explore biological phenomena. Acta Histochem. Cytoc. 40, 101–111.